Journal of Fluorine Chemistry 178 (2015) 34–39

Contents lists available at ScienceDirect

Journal of Fluorine Chemistry

journal homepage: www.elsevier.com/locate/fluor

Fluorine–fluorine type II versus π_F–π stacking interactions in the supramolecular organizations of extended thiophene derivatives end capped by imino-perfluorophenyl units

Chady Moussallem, Magali Allain, Charlotte Mallet, Frédéric Gohier, Pierre Frère*

Université d'Angers, MOLTECH-Anjou, UMR CNRS 6200, 2 boulevard Lavoisier, 49045 Angers cedex, France

ARTICLE INFO

Article history:
Received 20 March 2015
Received in revised form 17 June 2015
Accepted 19 June 2015
Available online 25 June 2015

Keywords:
Pentafluorophenyl unit
Aryl–perfluoroaryl interactions
Halogen bonds
Azomethine bonds
Conjugated systems

ABSTRACT

The solid state arrangements of extended thiophene derivatives associating pentafluorophenyl units linked via azomethine bonds are analyzed in terms of intermolecular interactions involving hydrogen and halogen bonds and $\pi-\pi_F$ interactions. It is shown that in the presence of the shortest conjugated systems, the structure is driven by F···F type II contacts giving orthogonal disposition while the lengthening of the conjugated backbone favors parallel arrangements via $\pi-\pi_F$ interactions.

1. Introduction

The discovery of the benzene–perfluorobenzene co-crystallization by Patrick and Prosper [1] initiated numerous studies aiming at a better understanding of the intermolecular interactions involved between aryl and perfluoroaryl groups [2–9]. Although the various factors that determine the role of the fluorine atoms in the intermolecular interactions are not yet fully mastered, several types of interactions can be considered: (i) $\pi-\pi F$ interactions between aryl and perfluoroaryl units that contribute to favor the stacking of the molecules in the materials, (ii) hydrogen bonds C–F···H–C that favor the lateral contacts and can also contribute to strengthen the pi-stacking, (iii) C–F···πF contacts induced by the polarization of the C–F bond and by the character globally positive in the center of the aromatic C_6F_5 ring, and (iv) F···F halogen bonds [5,9–16]. Owing to the small polarizability of the fluorine atoms, the F···F contacts should be weak and do not have any influence on the stacking mode in the crystal. Ramasubbu et al. classified the halogen bonds in two types depending on the angles θ_1 and θ_2 adopted between the C–X···X–C bonds (Fig. 1): type I when $\theta_1 \approx \theta_2$ and type II when $\theta_1 \approx 180^\circ$ and $\theta_2 \approx 90^\circ$ [17–20]. The interactions of type II are considered as stabilizing while the type I interactions are only a consequence of the stacking mode in the solid [21]. Generally the F···F contacts are type I and it is admitted that the F···F interactions do not participate in the supramolecular organization of the solid. Nevertheless it was demonstrated that when pentafluorophenyl or tetrafluorophenyl units were combined with acceptor groups, F···F type II interactions could intervene in the packing of the molecules in the crystal [22]. In the field of organic semiconducting materials, the insertion of perfluorophenyl units in conjugated systems has been exploited to control the electronic affinity and/or the packing mode of the conjugated backbone and thus to tune the electronic properties of the materials [3,4,23–27].

We have reported on the structural features of Donor–Acceptor–Donor type conjugated materials associating furan or thiophene cycles linked via azomethine bonds to pentafluorophenyl units [28,29]. We showed that the imino-perfluorophenyl units drive the packing modes in the solids via subtle balance between $\pi-\pi$ and donor–acceptor interactions. The preponderant roles of these intermolecular interactions were strongly dependent on the nature of the heterocycle and on the extended systems used as a spacer between the two external pentafluorophenyls units. In our continuing effort of studying the role of the imino-perfluorophenyl units on the stacking mode of hybrid heterocycle–perfluorophenyl structures, we report here on the structural features of the extended compounds **1**–**3**. We show that the structures are entirely driven by intermolecular interactions induced by the external phenyl or

---

* Corresponding author. Tel.: +33 241735063.
E-mail address: pierre.frere@univ-angers.fr (P. Frère).

http://dx.doi.org/10.1016/j.jfluchem.2015.06.018

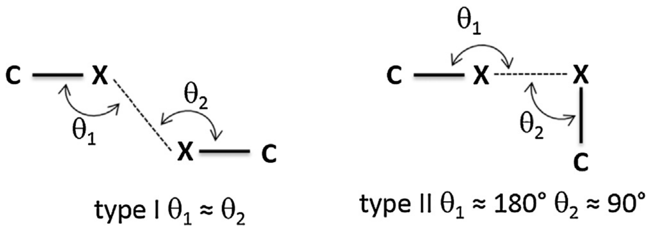

Fig. 1. The two types of halogen bonds.

perfluorophenyl units without any participation of the central thiophene cycle. Moreover depending on the length of the conjugated systems, a competition occurs between F···F interactions of type II and π_F–π stacking interactions.

2. Results and discussion

Compounds **1**–**3** were synthesized by condensation of 2,5-dicarbaldehyde thiophene **4** and 2,5-bis(3-oxo-1-propenyl)thiophene **5** with aniline or pentafluoroaniline (Scheme 1). Dialdehyde **5** was prepared by Wittig oxopropenylation with 1,3-dioxan-2-ylmethyltributylphosphorane on **4** [30]. Compound **1** was obtained by adding an excess of aniline to aldehyde **4** without solvent at room temperature [31]. The exothermic reaction led to a yellow solid which was washed with methanol to give **1** in 90% yield. Compounds **2** were obtained by condensation of aldehyde **4** and pentafluoroaniline in ethyl lactate as solvent at room temperature with a little amount of P_2O_5 (≈5 mol%) [32–35]. After 8 h stirring the mixture was poured in a water–methanol solution (50–50 vol.) to give a yellow precipitate. The solid was recrystallized from ethanol solution to give **2** in 70% yield. The same protocol with aldehyde **5** yielded compound **3** in small yield of 15%. The synthesis of compound **3** was also tested using microwave irradiation with a catalytic amount of P_2O_5 (10 mol%) in dichloromethane [28]. This method allowed to obtain **3** in 55% yield after chromatography on silica gel. The E–E configuration of the ethylenic bonds of **3** is demonstrated by the 15.6 Hz constant coupling in the ^{1}H NMR signal of the ethylenic bonds (Fig. S1 in supplementary data).

Electronic properties of compounds **1**–**3** have been analyzed by UV–vis spectroscopy and by cyclic voltammetry (CV) (Table 1). The UV–vis absorption spectra of compounds **1**–**3** in $CHCl_3$ exhibit broad band absorption bands (Fig. S2). Compounds **1** and **2** present maxima wavelength at 375 and 370 nm. The blue shift observed for **2** compared to **1** corresponds to an increase of the torsional angle of the azomethine bonds (Φ) with perfluorophenyl units (vide infra). As expected, the extension of the conjugated systems for **3** provokes a bathochromic shift of the absorption bands to reach a λ_{max} of 410 nm. The three compounds present an irreversible oxidation process respectively at 1.34, 1.52 and 1.28 V corresponding to the formation of a radical cation (Figs. S3–S5). Moreover **3** shows a second irreversible oxidation wave at 1.51 V due to the oxidation of $\mathbf{3}^{+\bullet}$ in dication $\mathbf{3}^{++}$. The extension of the conjugated systems by polyene units is known to favor the access to the dication state by decreasing the Coulombic repulsion between the positive charges. In reduction compounds **1**–**3** presents an irreversible wave respectively at −1.40, −1.30 and −1.32 V. The replacement of the phenyl by perfluorophenyl units between **1** and **2** increase the electron acceptor character leading to a rise both of oxidation and reduction potentials. The insertion of ethylenic bonds for **3** gives a modest effect on the reduction potential indicating that the electron acceptor character is mainly due to the iminoperfluorophenyl units [36,37].

Single crystals suitable for X-ray diffraction analysis are obtained for compounds **1**–**3** by slow evaporation of chloroform–ethanol solutions.

Compound **1** crystallizes in the monoclinic space group C2/c. The structure is defined from a half molecule which lies on a twofold axis. As shown in Fig. 2a, compound **1** has an E–E configuration for the azomethine junctions that present also a δ-syn configuration with the nitrogen atoms pointing in the same direction of sulfur atom. Such configuration of extended thiophene derivatives are often observed [38,39]. The lateral phenyl rings are not coplanar with the central conjugated system assuming a

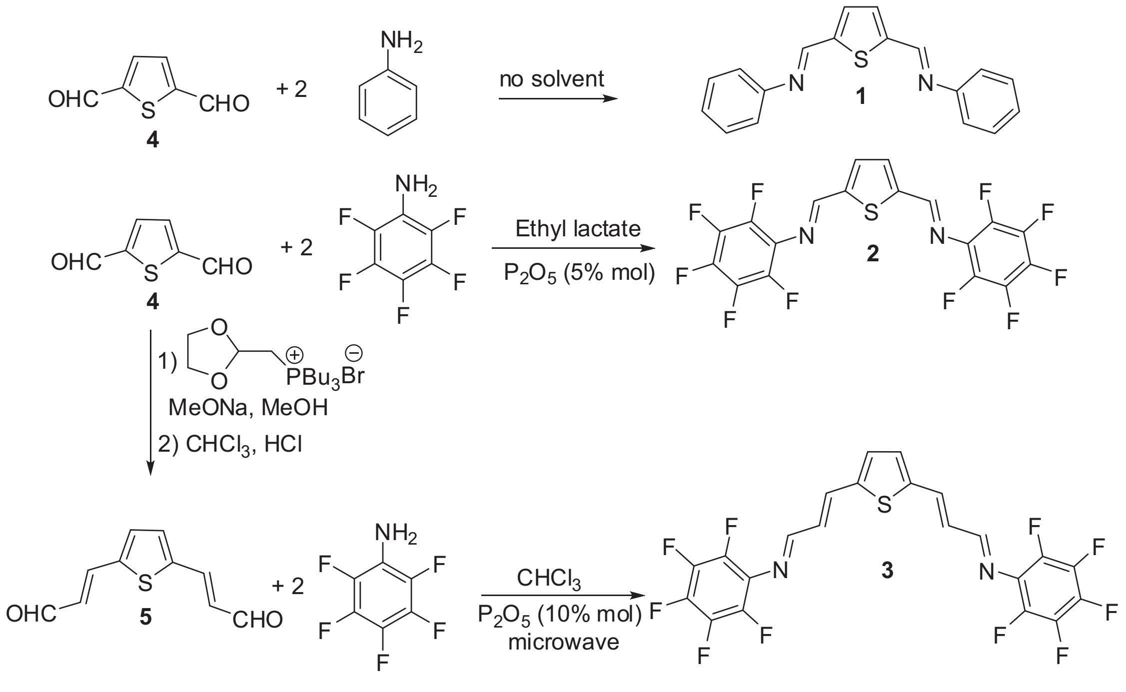

Scheme 1. Synthesis of compounds **1**–**3**.

Table 1
Torsional angle of azomethine bonds[a], electronic absorption[b] and cyclic voltammetry data[c] of compounds **1**–**3**.

Compound	$\Phi/(^\circ)$	λ_{max}/nm	Eox_1/V	Eox_2/V	$Ered_1$/V
1	35°	375	1.34	–	−1.45
2	45°	370	1.52	–	−1.30
3	35°	410	1.28	1.51	−1.32

[a] Calculated from the X-ray structure.
[b] 10^{-5} M in $CHCl_3$.
[c] 10^{-3} M in 0.1 M Bu_4NPF_6/CH_2Cl_2, v = 200 mV/s, reference AgCl/Ag.

torsional angle of 35° with respect to the thiophene cycle. The structure is iso-structural to the one obtained for furan analog [28]. The packing of the molecules is mainly defined by C–H···Ph interactions between the external phenyl cycles that present an edge to face arrangement (Figs. 2b and c). Such interactions lead to a stacking of the molecules along the *c* axis in a head to tail mode which strongly limits the contacts between the conjugated systems. As shown in Fig. 2c, the planes defined by the thiophene cycles are parallel and equidistant of 3.593(2) Å. There are few contacts between the thiophene cycles, the shortest distance between two atoms implying sulfur and carbon atoms of two adjacent thiophene cycles is of 3.601(2) Å. On the other hand, there is not any contact along the *a* and *b* axes between the columns of molecules.

Compound **2** crystallizes in the monoclinic space group Cc. The replacement of hydrogen atoms by fluorine atoms provokes a strong modification of the packing mode while the molecular structure is not strongly modified. The molecule **2** presents the same E–E configuration as **1** with a torsion angle between the perfluorophenyl rings and the imine bonds increasing to 45° (Fig. 3a). As shown in Fig. 3b, the molecules stack along the *b* axis with a juxtaposition of the thiophene cycles but without presenting any π–π interactions. Indeed the distance separating two planes defined by the thiophene cycle is of 3.83 Å with a S···S distance of 4.286(2) Å. The packing mode is defined by C–F···πF interactions between pentafluorophenyl rings that present a face to face arrangement with a slight shift allowing a fluorine atom to superimpose the center of the aromatic ring (Fig. 3c). The distance separating two benzene cores is of 3.2 Å. Between the columns of molecules, the structure exhibits type II F···F contacts with short distances $d_{F\cdots F}$ = 2.836(4) Å and angles of θ_1 = 86.7° and θ_2 = 156.3° (purple dotted lines in Figs. 3b and c) leading to quasi orthogonal arrangement between the two perfluorophenyl units. Moreover the contacts inter column are complemented by H···F contacts involving hydrogen atoms of the thiophene cycles with distances $d_{H\cdots F}$ = 2.70(7) Å (orange dotted lines in Fig. 3b) and habitual type I F···F contacts with distances of 2.852(5) Å and 2.881(5) Å (green dotted lines in Fig. 3b). By contrast with furan derivatives for which furan–perfluorophenyl interactions were observed, here there is no π-interaction between the thiophene and perfluorophenyl cycles for participating to the supramolecular organization.

Compound **3** crystallizes in the monoclinic space group C2/c. The structure is defined from a half molecule which lies on a twofold axis. The structure confirms the E–E configuration for the ethylenic protons and shows an E–E configuration for the imine bonds (Fig. 4a). The ethylenic and the imine bonds are in the plane defined by the central thiophene cycle while the external pentafluorophenyl groups present a torsional angle of 35° with the imine bonds.

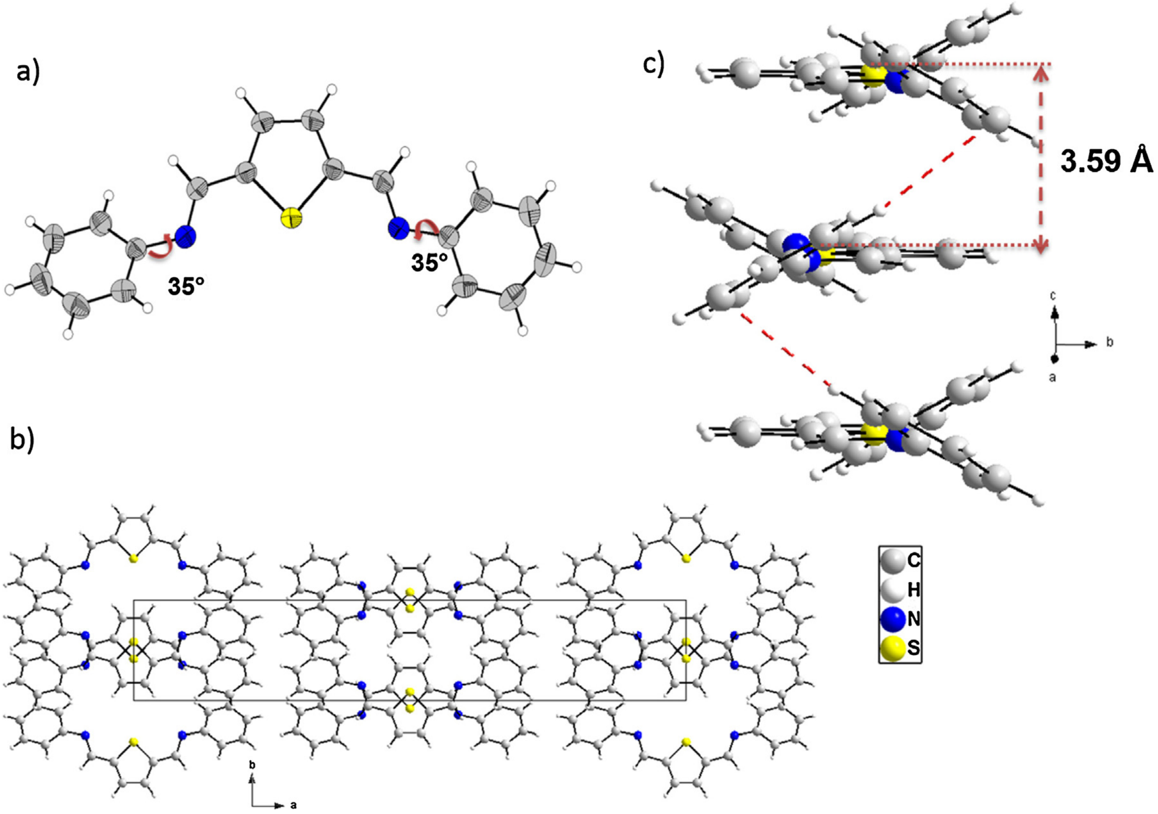

Fig. 2. X-ray structure of **1**. (a) Molecular structure of **1** with anisotropic displacement ellipsoid drawn at 50% probability level. (b) Crystal packing of **1** viewed along the *c* axis. (c) Stacking mode of molecules along the *c* axis, C–H···Ph interactions are shown in red dotted lines. (For interpretation of the references to color in this figure legend, the reader is referred to the web version of this article.)

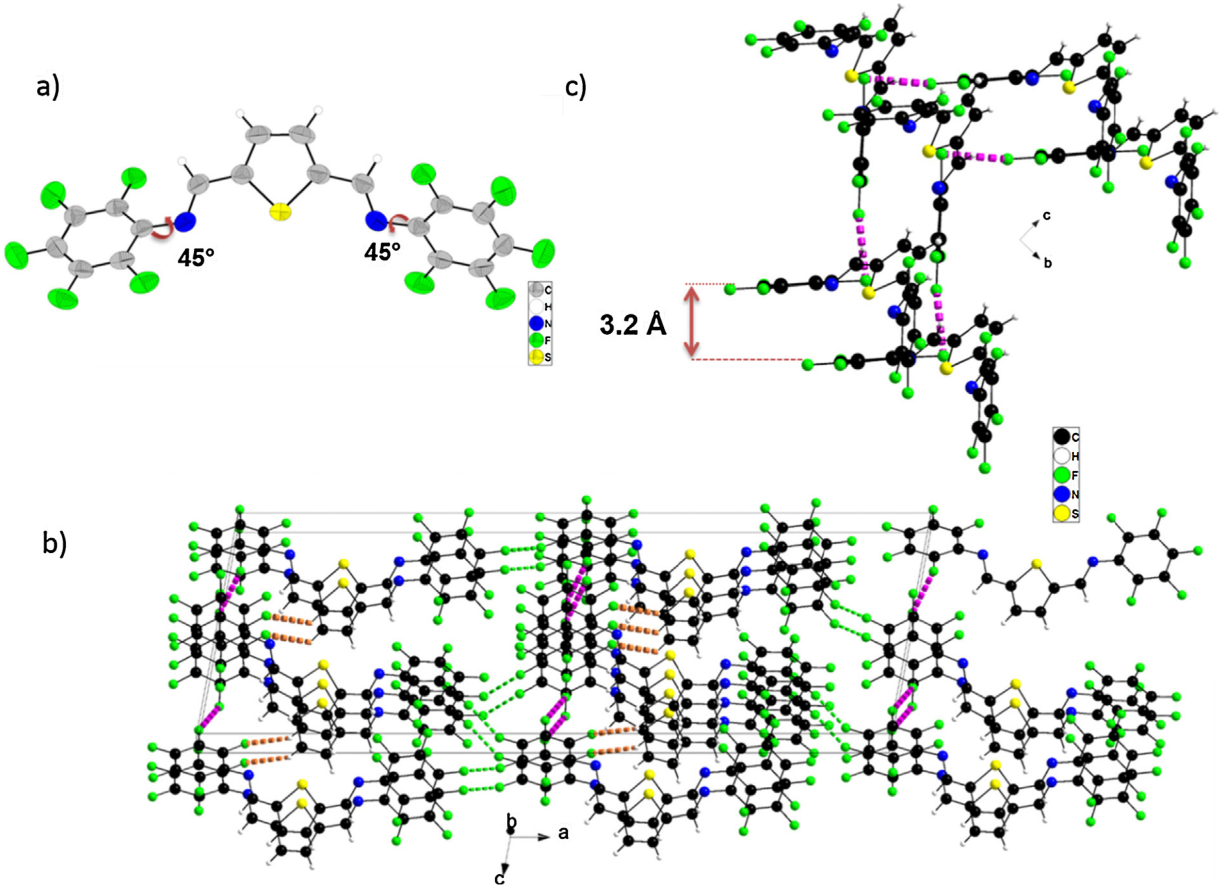

Fig. 3. X-ray structure of **2**. (a) Molecular structure of **2** with anisotropic displacement ellipsoid drawn at 50% probability level. (b) Crystal packing of **2** viewed along *b* axis, C–F···H–C contacts are presented in orange dotted lines and the type I F···F contacts in green dotted lines. (c) Stacking mode of molecules along the *b* axis showing the type II F···F contacts (purple dotted lines). (For interpretation of the references to color in this figure legend, the reader is referred to the web version of this article.)

The lengthening of the conjugated systems by the incorporation of ethylenic bonds between the central thiophene core and the external iminoperfluorophenyl units leads to increase the π contacts in the packing mode. As shown in Fig. 4b, the structure is built by some ribbons of molecules oriented along the *c* axis which stack along the *a* axis. The ribbons are linked themselves by C–H···F contacts with distances $d_{H\cdots F}$ = 2.523(3) Å (dotted orange line in Fig. 4b). Along the *a* axis, the molecules overlap by presenting an arrangement in which each molecule is in close contacts with four molecules, two below and two above (Fig. 4c). The short contacts are essentially due to interactions between carbon and fluorine atoms of the perfluorophenyl cycles and carbon and nitrogen atoms of the conjugated systems with interatomic distances ranging between 3.179(7) and 3.456(6) Å as shown by blue dotted lines in Fig. 4c. Thus the stacking mode in compound **3** mainly implicates π_F–π interactions combined with $\pi-\pi$ contacts.

In conclusion this comparative structural study between the compounds **1**–**3** well shows the primordial role of the external imino-perfluorophenyl groups to organize the packing arrangements in the crystals. The shortest structure **2** is dominated by F···F type II contacts completed by C–F···π_F interactions. Such organization is not in favor of a π-stacking mode. By lengthening the conjugated systems with ethylenic bonds in **3**, the importance of the C–F···π_F rises thus favoring parallel arrangement between the perfluorophenyl cycles, to the detriment of the orthogonal disposition imposed by F···F type II interactions, leading to a π-stacking mode.

3. Experimental

3.1. Synthesis

Dialdehyde derivatives **4** [40] and **5** [30] were synthesized as already described.

3.1.1. 2,5-Bis(phenyliminomethyl)thiophene **1** [31]

A slight excess of aniline was added to an erlenmeyer of 25 mL containing 1.0 g of dialdehyde **4** (7.1 mmol) at room temperature. The temperature rapidly raised thus allowing the liberation of vapor water. After 10 min, the brown solid obtained was purified by adding 3 mL of methanol. The solid was recovered by filtration, washed with 2 mL of methanol and dried in vacuo to give 1.9 g of compound **1** (90% yield).

Yellow pale solid, Mp = 204–206 °C.

^{1}H NMR (CDCl$_3$): 8.58 (s, 2H), 7.50 (s, 2H), 7.43–7.38 (m, 4H), 7.28–7.24 (m, 6H).

^{13}C NMR (CDCl$_3$): 152.5, 151.1, 146.5, 131.9, 129.4, 126.8, 121.3.

MS Maldi-tof: calcd. for $C_{18}H_{14}SN_2$ (M + H) 291.0956; found 291.0957.

Elemental analysis for $C_{18}H_{14}SN_2$: calcd. C 74.45, H 4.86, N 9.65; found 74.25, H 4.90, N 9.54.

3.1.2. 2,5-Bis(pentafluorophenyliminomethyl)thiophene **2**

Aldehyde **4** (52 mg, 0.37 mmol) and a catalytic amount of P_2O_5 were successively added to a solution of perfluoroaniline (200 mg, 1.1 mmol) in ethyl lactate (3 mL) at room temperature. After 8 h

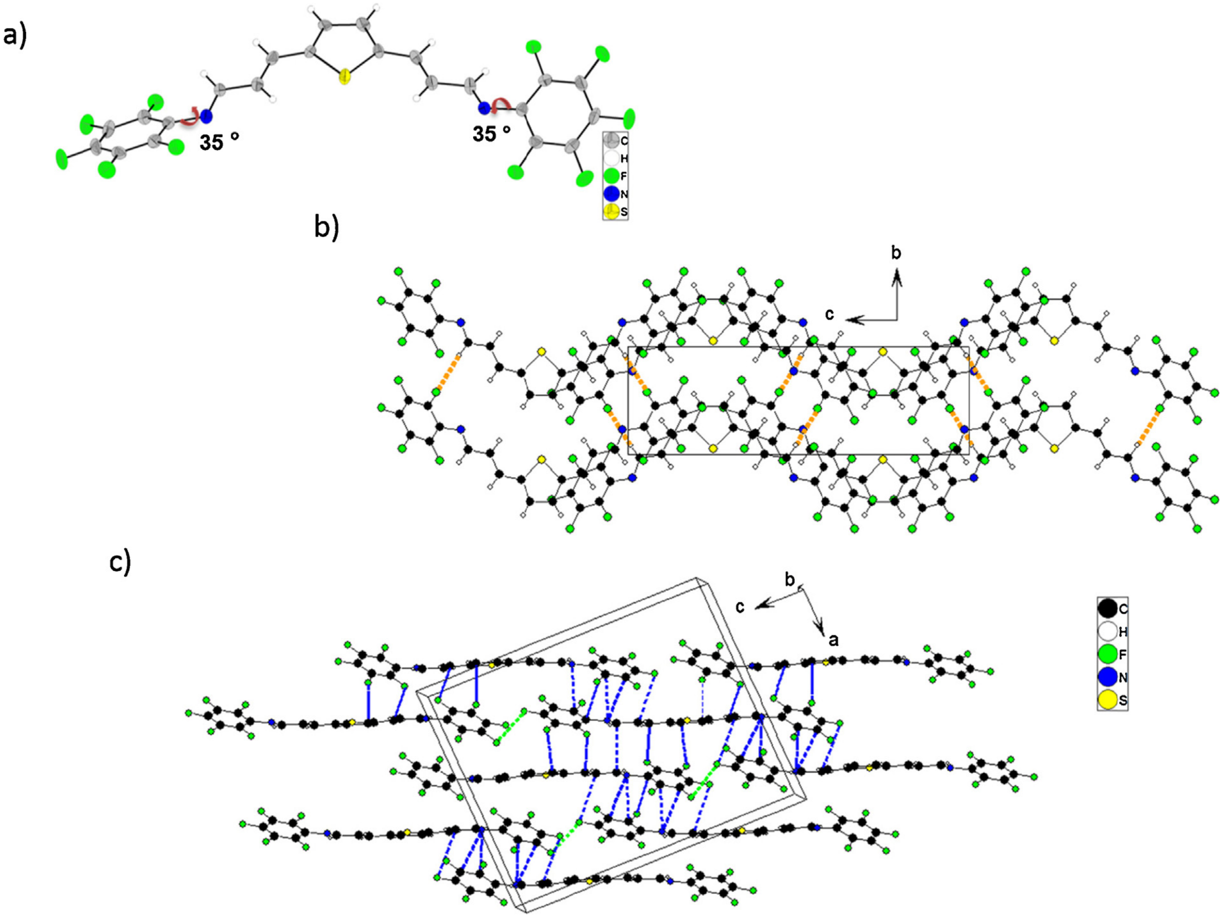

Fig. 4. X-ray structure of **3**. (a) Molecular structure of **3** with anisotropic displacement ellipsoid drawn at 50% probability level. (b) Partial crystal packing of **3** viewed along *a* axis C–F· · ·H–C contacts are presented in orange dotted lines. (c) Stacking mode of molecules along the *b* axis, shorter intermolecular distances are presented in blue dotted lines. (For interpretation of the references to color in this figure legend, the reader is referred to the web version of this article.)

stirring, the obtained precipitate was poured in a 10 mL of water-methanol (50/50 vol) solution. After filtration the solid was recovered, washed with methanol and dried under vacuum to give 120 mg of compound **2** (70% yield).

Yellow solid, Mp = 212–214 °C.

^{1}H NMR ($CDCl_3$): 8.77 (s, 2H), 7.60 (s, 2H).

^{13}C NMR ($CDCl_3$): 160.0, 146.9, 133.8.

^{19}F NMR ($CDCl_3$): −154.25 (dd, 4F, *J* = 21 Hz, *J* = 6 Hz), −162.15 (t, 2F, *J* = 21 Hz), −165.35 (td, 4F, *J* = 24 Hz, *J* = 6 Hz).

MS Maldi-tof: calcd. for $C_{18}H_4SN_2F_{10}$ (M + H) 471.0014; found 471.0013.

Elemental analysis for $C_{18}H_4SN_2$ F_{10}: calcd. C 45.97, H 0.86, N 5.96; found 45.54, H 0.67, N 5.80.

3.1.3. *2,5-Bis(pentafluorophenyliminoprop-1-enyl)thiophene* **3**

A 10 mL tube equipped with a magnetic stirring bar was filled with 115 mg of dialdehyde **5** (0.6 mmol), 320 mg of perfluoroaniline (1.7 mmol) in 3 mL of CH_2Cl_2 and 50 mg of P_2O_5. The tube was sealed with a rubber cap and irradiated three times for 10 min at 80 °C and under a pressure of 4.4 bar with a power reactor of 200 W. The mixture was cooled to room temperature, poured on 20 mL of water, extracted twice with CH_2Cl_2 (2 × 20 mL) and the organic phase was dried on $MgSO_4$. After evaporation of the solvent the residue was purified by a flash chromatography on silica gel in the presence of several drops of triethylamine (Petroleum ether/ CH_2Cl_2, 1/1) to give 173 mg (0.33 mmol) of compound **3** (55% yield).

Orange solid, Mp = 216–218 °C.

^{1}H NMR ($CDCl_3$): 8.35 (d, 2H, Himine, *J* = 8.9 Hz), 7.31 (d, 2H, Hethylenic, *J* = 15.6 Hz), 7.24 (s, 2H, Hthiophene), 6.97 (dd, 2H, Hethylenic, J_1 = 15.6 Hz and J_2 = 8.9 Hz).

^{13}C NMR (CD_3COCD_3): 166.4, 152.8, 139.1, 122.5, 113.7.

^{19}F NMR ($CDCl_3$): −155.35 (dd, 4F, *J* = 22 Hz, *J* = 6 Hz), −162.15 (t, 2F, *J* = 22 Hz), −165.35 (td, 4F, *J* = 24 Hz, *J* = 6 Hz).

MS Maldi-tof: calcd. for $C_{22}H_8SN_2F_{10}$ (M + H) 523.0327; found 523.0329.

Elemental analysis for $C_{22}H_8SN_2F_{10}$: calcd. C 50.58, H 1.54, N 5.36; found 50.46, H 1.68, N 5.12.

3.2. *X-ray structures*

X-ray single-crystal diffraction data of **1**–**3** were collected at 293 K for **1** and **2** and at 180 K for **3** on a BRUKER KappaCCD diffractometer for **1** and **3** and on a STOE IPDS diffractometer for **2**, both equipped with a graphite monochromator using MoKα radiation (λ = 0.71073 Å). The structures were solved by direct methods and refined by full matrix least squares techniques using SHELX97 package (G.M. Sheldrick, 1998). All non-H atoms were refined anisotropically and the H-atoms were found by Fourier difference for **1** and **2** or were included in the calculation without refinement for **3**. Absorption was corrected by gaussian technique for **1**, multi-scan technique for **2** and SADABS program (Bruker AXS area detector scaling and absorption correction, v2008/1, Sheldrick, G.M. (2008)) for **3**. Data collection details are found in Table 2.

Table 2
Data collection parameters for the resolved crystal structures of **1**–**3**.

Crystal	**1**	**2**	**3**
Formula	$C_{18}H_{14}N_2S$	$C_{18}H_4N_2F_{10}S$	$C_{22}H_8F_{10}N_2S$
Temperature	293	293	180
Molecular weight	290.37	470.29	522.36
Crystal system	Monoclinic	Monoclinic	Monoclinic
Space group	C2/c	Cc	C2/c
a (Å)	33.668(6)	34.915(4)	15.824(4)
b (Å)	5.995(1)	4.2860(2)	6.299(1)
c (Å)	7.4708(8)	11.5818(8)	20.023(2)
α (°)	90	90	90
β (°)	99.01(2)	100.39(1)	92.86(1)
γ (°)	90	90	90
V (Å^3)	1489.3(4)	1704.7(7)	1993.3(6)
Z	4	4	4
Crystal color	Yellow pale	Yellow	Orange
Crystal size (mm^3)	0.42 × 0.10 × 0.07	0.77 × 0.77 × 0.04	0.28 × 0.13 × 0.05
D_c (g/cm^3)	1.295	1.832	1.741
F (000)	608	928	1040
μ (/mm)	0.211	0.304	0.270
Transmission (max/min)	0.9862/0.9401	0.9881/0.6486	0.987/0.812
θ (min/max) (°)	4.48/28.07	3.56/25.76	2.04/27.65
Data collected	14,995	6090	10,385
Data unique	1773	3025	2265
R (int)	0.0667	0.0461	0.1331
Nb of parameters	124	296	159
R_1 [$I > 2\sigma(I)$]	0.0457	0.0526	0.0759
wR_2 [$I > 2\sigma(I)$]	0.0861	0.1369	0.1318
R_1 [all data]	0.0737	0.0614	0.1895
wR_2 [all data]	0.0978	0.1435	0.1768
GOF	1.113	1.000	1.056
Largest peak in final: difference (e/A^3)	0.195/−0.251	0.193/−0.186	0.447/−0.398

CCDC 1046004 (**1**), CCDC 1046003 (**2**), CCDC 1046005 (**3**) contains the supplementary crystallographic data of the structures.

Appendix A. Supplementary data

Supplementary data associated with this article can be found, in the online version, at http://dx.doi.org/10.1016/j.jfluchem.2015.06.018.

References

[1] C.R. Patrick, G.S. Prosser, Nature 187 (1960) 1021.
[2] J.H. Williams, Acc. Chem. Res. 26 (1993) 593–598.
[3] M.L. Renak, G.P. Bartholomew, S. Wang, P.J. Ricatto, R.J. Lachicotte, G.C. Bazan, J. Am. Chem. Soc. 121 (1999) 7787–7799.
[4] G.P. Bartholomew, X. Bu, G.C. Bazan, Chem. Mater. 12 (2000) 2311–2318.
[5] K. Reichenbacher, H.I. Suss, J. Hulliger, Chem. Soc. Rev. 34 (2005) 22–30.
[6] A. Collas, R. De Borger, T. Amanova, F. Blockhuys, CrystEngComm 13 (2011) 702–710.
[7] J.C. Collings, P.S. Smith, D.S. Yufit, A.S. Batsanov, J.A.K. Howard, T.B. Marder, CrystEngComm 6 (2004) 25–28.
[8] B.W. Gung, J.C. Amicangelo, J. Org. Chem. 71 (2006) 9261–9270.
[9] F. Cozzi, S. Bacchi, G. Filippini, T. Pilati, A. Gavezzotti, Chem. Eur. J. 13 (2007) 7177–7184.
[10] T.V. Rybalova, I.Y. Bagryanskaya, J. Struct. Chem. 50 (2009) 741–753.
[11] R. Berger, G. Resnati, P. Metrangolo, E. Weber, J. Hulliger, Chem. Soc. Rev. 40 (2011) 3496–3508.
[12] M. Stein, R. Berger, W. Seichter, J. Hulliger, E. Weber, J. Fluor. Chem. 135 (2012) 231–239.
[13] T.S. Thakur, M.T. Kirchner, D. Blaser, R. Boese, G.R. Desiraju, CrystEngComm 12 (2010) 2079–2085.
[14] R. Mariaca, N.-R. Behrnd, P. Eggli, H. Stoeckli-Evans, J. Hulliger, CrystEngComm 8 (2006) 222–232.
[15] S. Bacchi, M. Benaglia, F. Cozzi, F. Demartin, G. Filippini, A. Gavezzotti, Chem. Eur. J. 12 (2006) 3538–3546.
[16] F. Cozzi, S. Bacchi, G. Filippini, T. Pilati, A. Gavezzotti, CrystEngComm 11 (2009) 1122–1127.
[17] N. Ramasubbu, R. Parthasarathy, P. Murray-Rust, J. Am. Chem. Soc. 108 (1986) 4308–4314.
[18] M. Fourmigue, Curr. Opin. Solid State Mater. Sci. 13 (2009) 36–45.
[19] A. Priimagi, G. Cavallo, P. Metrangolo, G. Resnati, Acc. Chem. Res. 46 (2013) 2686–2695.
[20] F. Meyer, P. Dubois, CrystEngComm 15 (2013) 3058–3071.
[21] A.-L. Barrès, M. Allain, P. Frère, P. Batail, Isr. J. Chem. 54 (2014) 689–698.
[22] R.B.K. Siram, D.P. Karothu, T.N. Guru Row, S. Patil, Cryst. Growth Des. 13 (2013) 1045–1049.
[23] C.-Z. Li, Y. Matsuo, T. Niinomi, Y. Sato, E. Nakamura, Chem. Commun. 46 (2010) 8582–8584.
[24] A. Facchetti, M.H. Yoon, C.L. Stern, H.E. Katz, T.J. Marks, Angew. Chem. Int. Ed. 42 (2003) 3900–3903.
[25] D.J. Crouch, P.J. Skabara, J.E. Lohr, J.J.W. McDouall, M. Heeney, I. McCulloch, D. Sparrowe, M. Shkunov, S.J. Coles, P.N. Horton, M.B. Hursthouse, Chem. Mater. 17 (2005) 6567–6578.
[26] C. Videlot-Ackermann, H. Brisset, J. Zhang, J. Ackermann, S. Nénon, F. Fages, P. Marsal, T. Tanisawa, N. Yoshimoto, J. Phys. Chem. C 113 (2009) 1567–1574.
[27] S. Clement, F. Meyer, J. De Winter, O. Coulembier, C.M.L. Vande Velde, M. Zeller, P. Gerbaux, J.-Y. Balandier, S. Sergeyev, R. Lazzaroni, Y. Geerts, P. Dubois, J. Org. Chem. 75 (2010) 1561–1568.
[28] C. Mallet, M. Allain, P. Leriche, P. Frère, CrystEngComm 13 (2011) 5833–5840.
[29] C. Moussallem, M. Allain, F. Gohier, P. Frère, New J. Chem. 37 (2013) 409–415.
[30] T.M. Cresp, M.V. Sargent, P. Vogel, J. Chem. Soc., Perkin Trans. 1 (1974) 37–41.
[31] K. Tenza, M.J. Hanton, A.M.Z. Slawin, Organometallics 28 (2009) 4852–4867.
[32] J.S. Bennett, K.L. Charles, M.R. Miner, C.F. Heuberger, E.J. Spina, M.F. Bartels, T. Foreman, Green Chem. 11 (2009) 166–168.
[33] C. Moussallem, F. Gohier, C. Mallet, M. Allain, P. Frère, Tetrahedron 68 (2012) 8617–8621.
[34] C. Moussallem, O. Segut, F. Gohier, M. Allain, P. Frère, ACS Sustainable Chem. Eng. 2 (2014) 1043–1048.
[35] C.S.M. Pereira, V.M.T.M. Silva, A.E. Rodrigues, Green Chem. 13 (2011) 2658–2671.
[36] A. Benhamed-Gasmi, P. Frère, E.H. Elandaloussi, J. Roncali, J. Orduna, J. Garin, M. Jubault, A. Riou, A. Gorgues, Chem. Mater. 8 (1996) 2291–2297.
[37] P. Frère, J.M. Raimundo, P. Blanchard, J. Delaunay, P. Richomme, J.L. Sauvajol, J. Orduna, J. Garin, J. Roncali, J. Org. Chem. 68 (2003) 7264–7265.
[38] M.M. Bader, P.-T.T. Pham, E.H. Elandaloussi, Cryst. Growth Des. 10 (2010) 5027–5030.
[39] P. Frère, M. Allain, E.H. Elandaloussi, E. Levillain, F.X. Sauvage, A. Riou, J. Roncali, Chem. Eur. J. 8 (2002) 784–792.
[40] A. Seidler, J. Svoboda, V. Dekoj, J.V. Chocholoušová, J. Vacek, I.G. Stará, I. Starý, Tetrahedron Lett. 54 (2013) 2795–2798.